BIOCHEMISTRY
including biophysical chemistry & molecular biology

Article

pubs.acs.org/biochemistry

Fourier-Transform Infrared Study of the Photoactivation Process of *Xenopus* (6–4) Photolyase

Daichi Yamada,[†] Yu Zhang,[†] Tatsuya Iwata,[†,‡] Kenichi Hitomi,[§,∥] Elizabeth D. Getzoff,[§] and Hideki Kandori*[,†]

[†]Department of Frontier Materials, Nagoya Institute of Technology, Showa-ku, Nagoya 466-8555, Japan

[‡]Center for Fostering Young and Innovative Researchers, Nagoya Institute of Technology, Showa-ku, Nagoya 466-8555, Japan

[§]Department of Molecular Biology and Skaggs Institute for Chemical Biology, The Scripps Research Institute, La Jolla, California 92037, United States

[∥]Section of Laboratory Equipment, National Institute of Biomedical Innovation, 7-6-8, Saito-Asagi, Ibaraki, Osaka 567-0085, Japan

Supporting Information

ABSTRACT: Photolyases (PHRs) are blue light-activated DNA repair enzymes that maintain genetic integrity by reverting UV-induced photoproducts into normal bases. The flavin adenine dinucleotide (FAD) chromophore of PHRs has four different redox states: oxidized (FAD^{ox}), anion radical ($FAD^{\bullet -}$), neutral radical ($FADH^{\bullet}$), and fully reduced ($FADH^{-}$). We combined difference Fourier-transform infrared (FTIR) spectroscopy with UV–visible spectroscopy to study the detailed photoactivation process of *Xenopus* (6–4) PHR. Two photons produce the enzymatically active, fully reduced PHR from oxidized FAD: FAD^{ox} is converted to semiquinone via light-induced one-electron and one-proton transfers and then to $FADH^{-}$ by light-induced one-electron transfer. We successfully trapped $FAD^{\bullet -}$ at 200 K, where electron transfer occurs but proton transfer does not. UV–visible spectroscopy following 450 nm illumination of FAD^{ox} at 277 K defined the $FADH^{\bullet}$/$FADH^{-}$ mixture and allowed calculation of difference FTIR spectra among the four redox states. The absence of a characteristic C=O stretching vibration indicated that the proton donor is not a protonated carboxylic acid. Structural changes in Trp and Tyr are suggested by UV–visible and FTIR analysis of $FAD^{\bullet -}$ at 200 K. Spectral analysis of amide I vibrations revealed structural perturbation of the protein's β-sheet during initial electron transfer ($FAD^{\bullet -}$ formation), a transient increase in α-helicity during proton transfer ($FADH^{\bullet}$ formation), and reversion to the initial amide I signal following subsequent electron transfer ($FADH^{-}$ formation). Consequently, in (6–4) PHR, unlike cryptochrome-DASH, formation of enzymatically active $FADH^{-}$ did not perturb α-helicity. Protein structural changes in the photoactivation of (6–4) PHR are discussed on the basis of these FTIR observations.

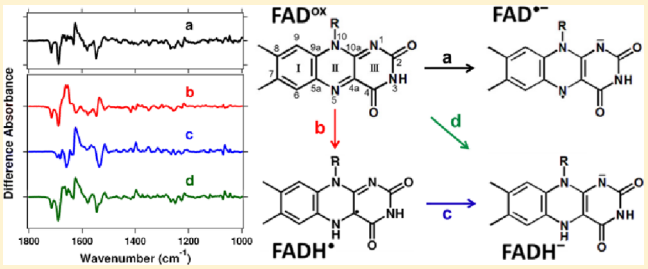

Ultraviolet (UV) components of sunlight are harmful to life because they trigger various chemical reactions inside cells. Organisms have developed diverse defense systems. Photolyases (PHRs) are unique DNA repair enzymes that maintain genetic integrity by reverting UV-induced photoproducts on DNA strands into normal bases with blue light (Figure 1).[1,2] Most prokaryotes have a single PHR that specifically repairs the cyclobutane pyrimidine dimer (CPD), whereas some higher eukaryotes possess an additional PHR that restores the pyrimidine-pyrimidone (6–4) photoproduct [(6–4) PP] to parental bases. The discovery of (6–4) PHR occurred 40 years after the first isolation of a CPD PHR gene.[3] Because of the greater structural complexity of (6–4) PP compared to that of CPD, the synthesis of DNA oligonucleotide substrates carrying a single (6–4) PP was more difficult. However, structural determination of (6–4) PHR provides insights into product recognition by the enzyme.[4,5]

The structures of (6–4) PHRs show an overall fold similar to that of CPD PHRs, consisting of α/β and α barrel domains connected with a unique long loop.[4,5] Flavin adenine dinucleotide (FAD) is the common chromophore for both PHRs. The chromophore is buried in the α barrel domain with the redox-active isoalloxazine ring sequestered from solvent. Reduced FAD is the active form for PHR catalysis. The oxidized FAD is a resting state in purified enzymes for (6–4) PHRs,[6] while most CPD PHRs stabilize $FADH^{\bullet}$.[1] Remarkably, PHRs have a system for regaining activity. In the presence of a reducing agent, buried FADs inside PHRs can be light-dependently reduced. PHRs have the tryptophan triad chain, considered to be important for this photoreduction, that links FAD to the protein surface. In *Escherichia coli* CPD PHR,

Received: April 25, 2012
Revised: June 27, 2012
Published: July 2, 2012

   dx.doi.org/10.1021/bi300530x | *Biochemistry* 2012, 51, 5774–5783

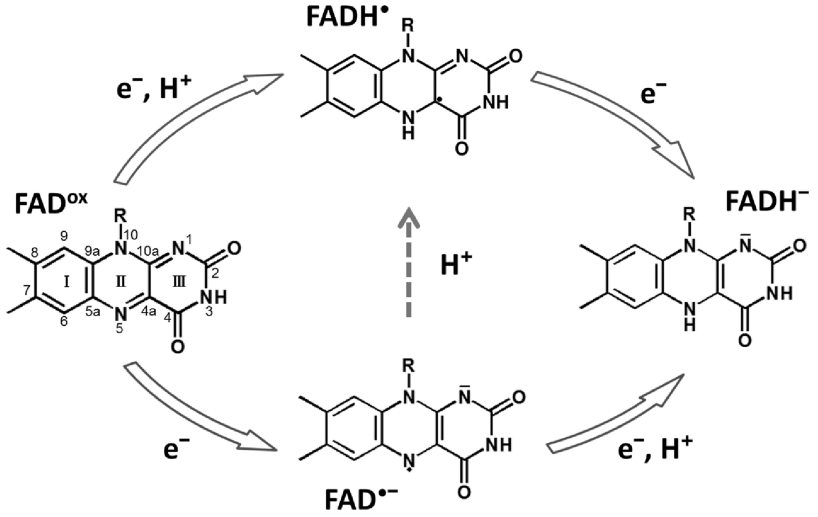

Figure 1. Four redox states of FAD in the CRY/PHR family. An oxidized form (FAD^{ox}) is the most stable species in *Xenopus* (6–4) PHR, insect CRY, and CRY-DASH from *Synechocystis* (SCRY-DASH). For activation of *Xenopus* (6–4) PHR, FAD^{ox} is first converted to a neutral radical form ($FADH^{\bullet}$) by light-induced one-electron and one-proton transfers (top pathway) and then into a fully reduced form ($FADH^{-}$) by light-induced one-electron transfer (top pathway).[1] In insect CRY, FAD^{ox} is converted to an anion radical form ($FAD^{\bullet-}$) by light-induced one-electron transfer (bottom pathway), and $FAD^{\bullet-}$ is highly stable.[14] In SCRY-DASH, FAD^{ox} is first converted to $FAD^{\bullet-}$ by light-induced one-electron transfer (bottom pathway) and then into a fully reduced form ($FADH^{-}$) by light-induced one-electron and one-proton transfer (bottom pathway).[18]

substitution of the outside tryptophan of the triad chain disturbs this process.[7,8] (6–4) PHRs structurally conserve the tryptophan triad chain with some modification. Two photons are needed for this photactivation: the oxidized form of FAD is first converted to the semiquinone by light-induced one-electron and one-proton transfers and then to the reduced form, $FADH^{-}$, by light-induced one-electron transfer. When the reduced enzyme absorbs another photon in the presence of the (6–4) PP, the transfer of an electron from $FADH^{-}$ to the photoproduct initiates the repair process.[6,9]

Light-induced difference Fourier-transform infrared (FTIR) spectroscopy is a powerful, sensitive, and informative method for studying structure–function relationships in photoreceptive proteins.[10−12] Recently, we applied FTIR spectroscopy to full-length *Xenopus laevis* (6–4) PHR and authentic DNA carrying a single (6–4) PP to gain insights into the reaction mechanisms.[13] Consequently, we successfully obtained difference FTIR spectra that correspond to the photoactivation (light-induced FAD reduction) process and light-dependent DNA repair reactions of (6–4) PHR. In addition, time-dependent illumination of samples with different enzyme:substrate stoichiometries distinguished signals characteristic of structural changes in the protein and the DNA resulting from binding and catalysis. This improved our understanding of the molecular mechanisms of (6–4) PHR in atomic detail, particularly with regard to enzymatic catalysis.

It should be noted, however, that the reported difference FTIR spectrum of photoactivation is only between fully oxidized (FAD^{ox}) and fully reduced ($FADH^{-}$) forms. On the other hand, the photoactivation process of (6–4) PHR is more complex, where two photons are needed from FAD^{ox}, a resting state. FAD^{ox} is first converted to $FADH^{\bullet}$ by light-induced one-electron and one-proton transfers [proton transfer-coupled electron transfer (PCET)] and then to $FADH^{-}$ by light-induced one-electron transfer.[6] This indicates the presence of a semiquinoid neutral radical ($FADH^{\bullet}$) as an intermediate. In addition, if the electron and proton transfer reaction is separated in the primary PCET, an anion radical intermediate ($FAD^{\bullet-}$) may be captured. This actually happens for insect cryptochrome, in which $FAD^{\bullet-}$ is stable even at room temperature.[14] It is known that the amino acid closest to the N_5 position of FAD is the determinant of the stability of $FAD^{\bullet-}$, and insect cryptochrome (CRY) has Cys at this position.[15] Most members of the PHR/CRY family possess Asn or Asp, where $FAD^{\bullet-}$ is unstable and $FADH^{\bullet}$ is easily formed. It is likely that the hydrogen bonding network anchored by Asn or Asp in this vicinity acts for the efficient transfer of a proton to FAD.[16] In CRY-DASH from *Synechocystis*,[17] mutation of the corresponding Asn to Cys stabilized $FAD^{\bullet-}$.[18] *Xenopus* (6–4) PHR also possesses Asn at this position, and a lack of observation of $FAD^{\bullet-}$ at room temperature (Figure 2) is predicted. Here we studied the detailed activation process of *Xenopus* (6–4) PHR, i.e., from FAD^{ox} to $FADH^{-}$, using UV–visible and FTIR spectroscopy. By selecting the temperature and illumination wavelength, we are able to obtain difference FTIR spectra of each of four redox states: FAD^{ox}, $FAD^{\bullet-}$, $FADH^{\bullet}$, and $FADH^{-}$.

MATERIALS AND METHODS

Sample Preparation. In our previous paper, *Xenopus* (6–4) PHR was expressed in *E. coli* as a fusion protein with glutathione *S*-transferase (GST) at the N-terminus, which was cleaved with thrombin after the purification by glutathione Sepharose 4B resin (GE Healthcare).[13,19] However, the amount of purified protein was small (0.26 mg from a 1 L culture), which is disadvantageous for our future study using isotope labeling and mutation. Therefore, we used the His tag system in this study as follows.

The gene of *Xenopus* (6–4) PHR containing a His tag at the N-terminus was inserted at the NdeI and XhoI sites of the pET-28a expression vector (Novagen). *E. coli* BL21(DE3) transformed with the vector was added to 1 L of LB medium in a 3 L flask and grown at 25 °C until the OD_{660} reached 1.25–1.5. The culture was then adjusted to 1 mM isopropyl β-D-thiogalactopyranoside, incubated for 24 h, and then harvested by centrifugation. The pellet was frozen at −80 °C, thawed,

dx.doi.org/10.1021/bi300530x | *Biochemistry* 2012, 51, 5774–5783

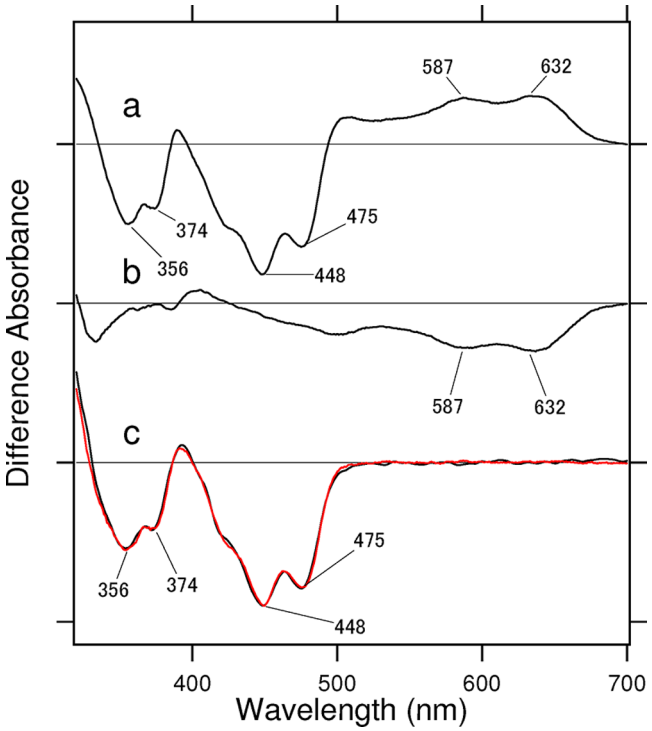

Figure 2. Light-induced difference UV−visible spectra of the redissolved sample of *Xenopus* (6−4) PHR at 277 K. (a) Difference spectrum from a 450 nm light illumination (an interference filter) of FAD^{ox} for 4 min, where $FADH^{\bullet}$ was formed as shown by broad positive absorption at 500−700 nm. Note that $FADH^{-}$ was also produced under these illumination conditions, and the relative amounts of $FADH^{\bullet}$ and $FADH^{-}$ produced were estimated to be 0.49 and 0.51, respectively, by using their individual molar extinction coefficients (see the text). (b) After the illumination described for panel a, the sample was illuminated with >550 nm light for 1 min, which provided the $FADH^{-}$ minus $FADH^{\bullet}$ difference spectrum. (c) Sum of spectra a and b (red line) that coincides with the $FADH^{-}$ minus FAD^{ox} difference spectrum obtained by illumination of FAD^{ox} at >450 nm for 4 min (black line). One division of the *y*-axis corresponds to 0.04 absorbance unit.

resuspended in lysis buffer [50 mM sodium phosphate, 200 mM NaCl, and 5 mM imidazole (pH 8.0)], and sonicated. Cell debris was removed from the lysate by ultracentrifugation at 17700 rpm for 1 h. The cell-free extract was loaded onto a TALON Metal Affinity Resin column (TAKARA), and the fusion protein was eluted with elution buffer [50 mM sodium phosphate, 200 mM NaCl, and 500 mM imidazole (pH 8.0)]. The sample was then applied to a HiTrap Heparin HP column (GE Healthcare) and eluted with a linear gradient from 0.2 to 1 M NaCl. The protein expressed in *E. coli* does not bind a second chromophore, such as MTHF.[6] A 5 L culture of *E. coli* yielded 11 mg of (6−4) PHR, which is 8.5 times larger than the amount produced by the previous preparation method using the GST tag system. When the purified (6−4) PHR was stored, it was kept at −80 °C in 50 mM Tris-HCl buffer (pH 8.0) containing 200 mM NaCl and 5% (w/v) glycerol.

We used redissolved samples for UV−visible and FTIR spectroscopy, as established in the previous study.[13] First, we placed 2 μL of the sample solution containing 1 mM (6−4) PHR in 50 mM Tris-HCl buffer (pH 8.0) and 200 mM NaCl on an IR window (BaF_2) and dried it. We then placed 0.4 μL of the 50 mM Tris-HCl buffer (pH 8.0) containing 200 mM NaCl directly onto the dried film and sandwiched that window with another IR window. (6−4) PHR in D_2O was prepared by diluting the (6−4) PHR with the same buffer prepared in D_2O and concentrating with the Amicon YM-30 device (Millipore) three times. The same procedure was used except for using D_2O buffer for the preparation of redissolved samples.

UV−Visible and FTIR Spectroscopy. UV−visible and FTIR spectra of the redissolved samples were measured using V-550DS (JASCO) and FTS-7000 (DIGILAB) spectrophotometers, respectively, as reported previously.[13,19−21] Samples were placed in an Oxford Optistat-DN cryostat mounted in the spectrophotometer, which was also equipped with a temperature controller (ITC-4, Oxford). The illumination source was a high-power 300 W xenon lamp (MAX-302, ASAHI SPECTRA), and illumination at 450 nm (MZ0450, ASAHI SPECTRA), >550 nm (XF593, ASAHI SPECTRA), 300−400 nm (C-40B, Toshiba), or >450 nm (VY-45, Toshiba) was provided. The FTIR spectra were constructed from 128 interferograms with a spectral resolution of 2 cm^{-1}. The difference spectrum was calculated by subtracting the spectrum recorded before illumination from the spectrum recorded after illumination. Six to eight difference spectra obtained in this way were averaged for each difference spectrum.

In this study, the N-terminal His tag was not removed, and we thus tested whether His-tagged *Xenopus* (6−4) PHR provides spectra similar to those in the previous report.[13] Figure S1 of the Supporting Information compares light-induced difference FTIR spectra of His-tagged *Xenopus* (6−4) PHR in this study (red line) with the reported spectra (black line) for photoactivation (Figure S1a of the Supporting Information, $FADH^{-}$ minus FAD^{ox}) and photorepair [Figure S1b of the Supporting Information; repaired DNA minus (6−4) PP]. Red and black spectra coincide well, and the reproduced spectra demonstrate identical structural changes for the two different preparations.

RESULTS

Capturing $FADH^{\bullet}$: Light-Induced Difference UV−Visible and FTIR Spectra of (6−4) PHR at 277 K. We previously illuminated the redissolved sample of FAD^{ox}, the resting state of (6−4) PHR, with >450 nm light and obtained $FADH^{-}$ at 277 K.[13] Under such photoactivation conditions, we did not detect significant absorption near 600 nm, characteristic of $FADH^{\bullet}$. In contrast, we observed the appearance of a broad absorption at 500−700 nm and 277 K by illuminating FAD^{ox} of (6−4) PHR (redissolved sample) for 4 min at 450 nm, by using an interference filter (Figure 2a). This clearly shows formation of $FADH^{\bullet}$ at 277 K.[22] It should be noted that the photoproduct is not only $FADH^{\bullet}$ but also $FADH^{-}$. On the other hand, the absence of the $FAD^{\bullet-}$ specific 350−400 nm bands on the positive side implies no accumulation of $FAD^{\bullet-}$.[14] Thus, the result in Figure 2a can be interpreted as follows; illumination converts FAD^{ox} into $FADH^{\bullet}$ by coupled electron and proton transfer reactions, with some species being further reduced to $FADH^{-}$. According to the extinction coefficients of various redox states of *Xenopus* (6−4) PHR reported by Schleicher et al.,[22] relative absorbances of 1, 0.54, and 0.24 at 450 nm and 0, 0.40, and 0 at 580 nm were determined for FAD^{ox}, $FADH^{\bullet}$, and $FADH^{-}$, respectively. From these values, we estimated the positive components of the spectrum in Figure 2a to be 49% $FADH^{\bullet}$ and 51% $FADH^{-}$. These values will be used to obtain the "pure" difference FTIR spectra below.

After the spectrum of Figure 2a was obtained by 450 nm light illumination, we continuously illuminated the sample for 1 min

dx.doi.org/10.1021/bi300530x | *Biochemistry* 2012, 51, 5774−5783

with >550 nm light, which is absorbed by only FADH• (Figure 2b).[22] As a result, FADH• is photoconverted as evidenced by a negative broad band at 500−700 nm. FAD^{ox} is involved neither as the reactant nor as the product, as seen from the absence of its characteristic peaks at 448 and 475 nm in Figure 2b. It is likely that FADH• is dominantly converted into $FADH^-$ by an electron transfer.[7] This interpretation is further supported by the spectral analysis in Figure 2c. The sum of spectra a and b in Figure 2 (red line in Figure 2c) coincides very well with the $FADH^-$ minus FAD^{ox} spectrum (black line in Figure 2c) obtained by illuminating FAD^{ox} with >450 nm light. Both spectra agree with the reported $FADH^-$ minus FAD^{ox} spectrum.[13] It should be noted that visible absorption at 500−700 nm is characteristic of cation or neutral radicals of Trp and Tyr,[23−25] as well as flavins. However, such signals are not apparent in the present static measurements at 277 K, as it is evident from the $FADH^-$ minus FAD^{ox} spectrum coinciding with the baseline at >500 nm (Figure 2c). The 500−700 nm band present in the static measurements at 277K (Figure 2a) instead represents the FADH• intermediate produced during the reduction of FAD^{ox} to $FADH^-$.

Using identical sample and experimental conditions from UV−visible spectroscopy, we next applied difference FTIR spectroscopy to the redissolved sample of (6−4) PHR. Figure 3a shows the light-induced difference FTIR spectrum upon illumination of FAD^{ox} of (6−4) PHR at 450 nm. From the analysis in the UV−visible region (Figure 2a), the product is a mixture of 49% FADH• and 51% $FADH^-$. Figure 3b represents the difference FTIR spectrum obtained by illumination with >550 nm light, matching the illumination conditions used for Figure 2b. Therefore, Figure 3b corresponds to the $FADH^-$ minus FADH• spectrum. The smaller amplitude in Figure 3b relative to that in Figure 3a probably results from photoconversion of half the FADH•. The red spectrum in Figure 3c is the sum of spectra a and b of Figure 3, which coincides very well with the $FADH^-$ minus FAD^{ox} spectrum (black line in Figure 3c) obtained by illumination of FAD^{ox} with >450 nm light. Both spectra also coincide with the reported $FADH^-$ minus FAD^{ox} difference FTIR spectrum.[13]

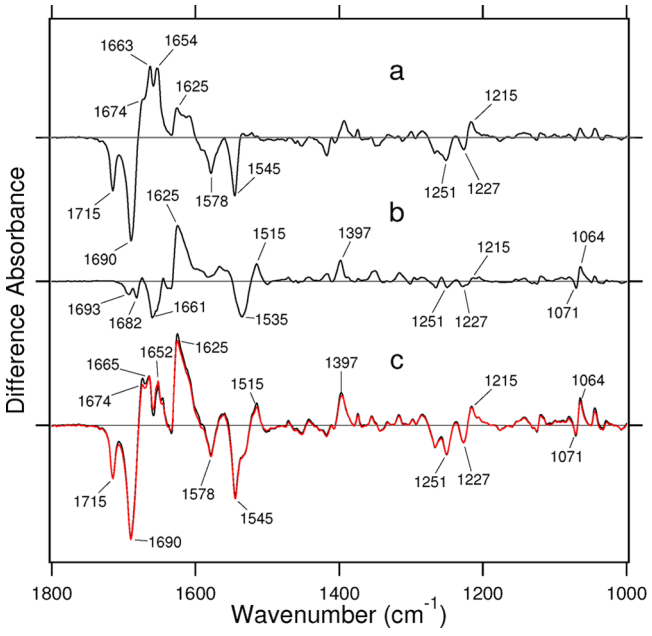

Figure 3. Light-induced difference FTIR spectra of the redissolved sample of *Xenopus* (6−4) PHR at 277 K. (a) Difference spectrum generated by 450 nm light illumination (an interference filter) of FAD^{ox} for 4 min (condition identical to that for Figure 2a), where the product consists of 49% FADH• and 51% $FADH^-$. (b) After the illumination for panel a, the sample was illuminated with >550 nm light for 1 min (condition identical to that for Figure 2b), which provided the $FADH^-$ minus FADH• difference spectrum. (c) Sum of spectra a and b (red line) that coincides with the $FADH^-$ minus FAD^{ox} difference spectrum obtained by illumination of FAD^{ox} with >450 nm light for 4 min (black line). One division of the *y*-axis corresponds to 0.008 absorbance unit.

Isolation of $FAD^{•-}$: Light-Induced Difference UV−Visible and FTIR Spectra of (6−4) PHR at 200 K. Conversion from FAD^{ox} to FADH• occurs through both one-electron and one-proton transfer reactions. If only an electron transfer takes place, $FAD^{•-}$ is produced from FAD^{ox}. The stability of this anion radical is highly dependent on the protein environment. In particular, the amino acid closest to the N_5 position of FAD is important.[15] In insect specific CRY, functioning as the photoreceptor of the circadian clock, Cys near N_5 favors $FAD^{•-}$ even at room temperature.[14] However, most members of the PHR/CRY family possess Asn or Asp and typically stabilize FADH• rather than $FAD^{•-}$.[23] A hydrogen bonding network anchored to FAD N_5 by Asn or Asp likely promotes efficient proton transfer. In *Synechocystis* CRY-DASH, another PHR homologue, mutation of the corresponding Asn to Cys stabilized $FAD^{•-}$.[18] (6−4) PHRs also possess Asn at this position, and $FAD^{•-}$ is not detected in *Xenopus* (6−4) PHR at room temperature (Figure 2), consistent with the previous reports.[13] However, one might expect separation of the electron and proton transfers by lowering temperature, and that was indeed the case.

At 200 K, the light-induced difference UV−visible spectrum (Figure 4) upon illumination of FAD^{ox} of (6−4) PHR exhibits a positive peak at ∼380 nm, which is characteristic of the difference spectrum between $FAD^{•-}$ and FAD^{ox}.[18] This spectrum indicates that $FAD^{•-}$ is formed and stable in *Xenopus* (6−4) PHR at low temperatures, but neither FADH• nor $FADH^-$ accumulates. At 200 K, a broad positive feature can be observed at 500−700 nm, yet the analysis in Figure S2 of the

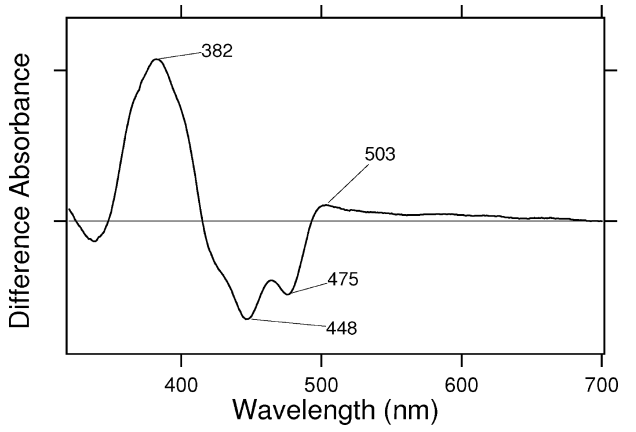

Figure 4. Light-induced difference UV−visible spectra of the redissolved sample of *Xenopus* (6−4) PHR at 200 K. FAD^{ox} was illuminated with 300−400 nm light for 20 min, and its difference spectrum is entirely different from Figure 2a. A positive peak is characteristic of the formation of $FAD^{•-}$. One division of the *y*-axis corresponds to 0.015 absorbance unit.

dx.doi.org/10.1021/bi300530x | *Biochemistry* 2012, 51, 5774−5783

Supporting Information shows that, at most, the level of $FADH^{\bullet}$ is <5%. Thus, the spectral feature at 500−700 nm cannot be explained by $FADH^{\bullet}$ alone (Figure S2 of the Supporting Information) but likely indicates the involvement of cation or neutral radicals of Trp and/or Tyr in the positive side of Figure 4. The formation of a Trp cation radical visible at 200 K would be consistent with an important role for the tryptophan triad chain in the electron transfer reaction: if the farthest Trp donates the electron to FAD, then the difference UV−visible spectrum (Figure 4) would contain the signal of the Trp cation radical. Previous pulsed radiolysis studies reported that cation and neutral radicals of Trp show absorption maxima at 560 and 510 nm,[25] which are in good agreement with the positive spectral feature (Figure 4). The molar extinction coefficients of cation (ε_{510} = 2300 M^{-1} cm^{-1}) and neutral (ε_{560} = 3000 M^{-1} cm^{-1}) radicals of Trp are ∼4−5 times smaller than that of FAD^{ox} in (6−4) PHR (ε_{450} = 11200 M^{-1} cm^{-1}).[9] Thus, low-temperature UV−visible spectroscopy might suggest the presence of the electron donor, possibly Trp from the triad. In contrast, in the case of *S*CRY-DASH, DTT was needed for the conversion from FAD^{ox} to $FAD^{\bullet-}$, where the broad positive feature at 500−700 nm was absent.[18] This observation strongly supports our interpretation. Because UV−visible difference spectroscopy established the experimental conditions for trapping $FAD^{\bullet-}$, we then applied FTIR spectroscopy at 200 K.

Light-Induced Difference FTIR Spectra of the Four Redox States of (6−4) PHR. Figure 5a corresponds to the $FAD^{\bullet-}$ minus FAD^{ox} difference FTIR spectrum measured at 200 K. Then, the $FADH^{\bullet}$ minus FAD^{ox} difference FTIR spectrum (Figure 5b) was obtained by subtracting the spectrum in Figure 3c from that in Figure 3a using the result of the UV−visible analysis (Figure 2a, 49% $FADH^{\bullet}$ and 51% $FADH^{-}$ as the product). The $FADH^{-}$ minus $FADH^{\bullet}$ difference FTIR spectrum in Figure 5c was reproduced from Figure 3b after the amplitude had been scaled (divided by 0.49). The $FADH^{-}$ minus FAD^{ox} difference FTIR spectrum in Figure 5d was reproduced from Figure 3c. In this way, we were able to obtain difference FTIR spectra among four redox states. It should be noted that, except for Figure 5c, the scale of the amplitude in Figure 5 is normalized for the FAD^{ox} specific negative band at 1715 cm^{-1}.[13] The blue spectra in Figure 5 exhibit identical measurements in D_2O.

Figure 5 shows that the bands at 1489, 1535, and 1397 cm^{-1} are specific to $FAD^{\bullet-}$, $FADH^{\bullet}$, and $FADH^{-}$, respectively, and can therefore be used as marker bands for future analysis. Frequencies of FAD^{ox} at 1715, 1690, 1578, and 1545 cm^{-1} (negative bands in Figure 5a,b,d) can be ascribed to the C_4═O, C_2═O, C_{4a}═N_5, and C_{10a}═N_1 stretching vibrations of flavin, respectively.[26−31] A previous theoretical study suggested that the 1625 cm^{-1} band of $FAD^{\bullet-}$ (Figure 5a) and the 1535 cm^{-1} band of $FADH^{\bullet}$ (Figure 5b) originate from C_2═O and C_{10a}═N_1 stretching vibrations of flavin, respectively.[32,33] Thus, strong peaks can be assigned for the vibrations of flavin, but vibrations of protein are possibly involved in the difference spectra, as well.

Protonated Carboxylic COOH Stretching Vibrations at 1800−1700 cm^{-1}. C═O stretching vibrations of protonated carboxylic acids appear in the 1800−1700 cm^{-1} region and are spectrally downshifted by 5−15 cm^{-1} in D_2O.[34] Because there are no other vibrations in this region except for the C_4═O stretching vibration of flavin, detailed analysis of protonated carboxylic acids is possible. We observed only a negative peak at 1715 cm^{-1}, which shifted to 1714 cm^{-1} in D_2O (Figure 5a,b,d). As mentioned, the FAD^{ox} specific band originates from the C_4═O stretching vibration of the isoalloxazine ring.[26] The lack of other bands indicates that there are no structural changes for protonated carboxylic acids among four redox states. It should be noted that one proton is gained by the flavin from FAD^{ox}/$FAD^{\bullet-}$ to $FADH^{\bullet}$/$FADH^{-}$. A protonated carboxylic acid is a good candidate for the proton donor, and in fact, for photoreduction of plant CRY, a negative FTIR band at 1735 cm^{-1} suggested that a carboxylic acid is the FAD proton donor.[35] Unlike plant CRY, in the case of (6−4) PHR, protonated carboxylic acid is not the proton donor.[13] Consistent with the FTIR results, plant CRY anchors the redox-active FAD N_5 position with a hydrogen bond to the carboxylic acid Asp,[36] whereas PHRs conserve this position as Asn.[5]

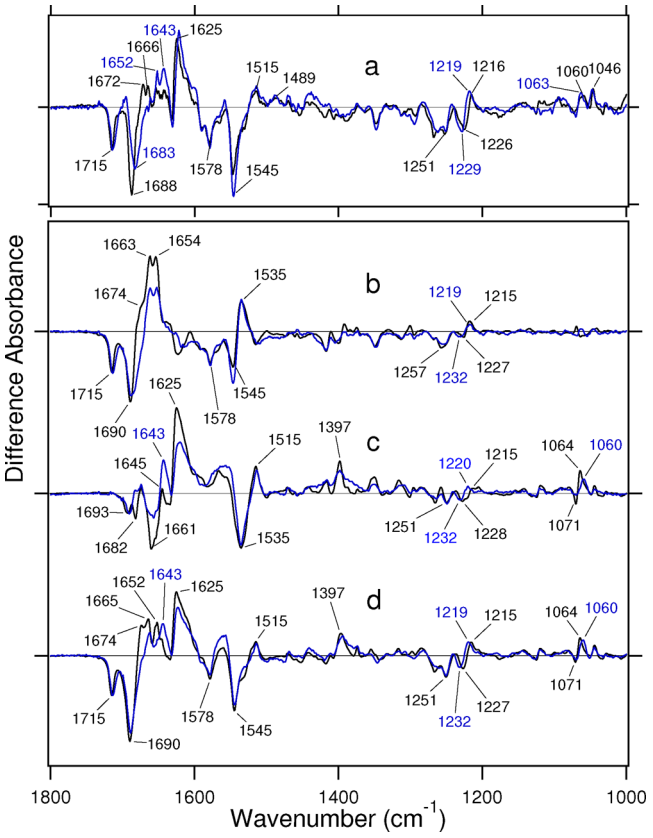

Figure 5. Light-induced difference FTIR spectra of the redissolved sample of *Xenopus* (6−4) PHR in H_2O (black line) and D_2O (blue line). (a) FAD^{ox} was illuminated with 300−400 nm light for 20 min at 200 K (condition identical to that of Figure 4), and light-minus-dark difference spectra correspond to the $FAD^{\bullet-}$ minus FAD^{ox} spectra. The obtained spectra were magnified 4.05-fold, so that the negative band at 1715 cm^{-1} exhibits the same amplitude as that in the $FADH^{-}$ minus FAD^{ox} spectrum (d). (b) $FADH^{\bullet}$ minus FAD^{ox} spectra calculated from those in panels a and c of Figure 3 (black line) with the contribution of $FADH^{-}$ removed (see the text). The calculated spectra were magnified 2.04-fold, so that the negative band at 1715 cm^{-1} exhibits the same amplitude as that in the $FADH^{-}$ minus FAD^{ox} spectrum (d). (c) $FADH^{-}$ minus $FADH^{\bullet}$ spectra reproduced from Figure 3b, but with the amplitude magnified 2.04-fold to show the same molar reaction. (d) $FADH^{-}$ minus FAD^{ox} spectra reproduced from the black line in Figure 3c. From the normalizations shown above, panels a−d show the same molar reaction with each other. One division of the *y*-axis corresponds to 0.0065 (above) or 0.012 (below) absorbance unit.

dx.doi.org/10.1021/bi300530x | *Biochemistry* 2012, 51, 5774−5783

Involvement of Trp and/or Tyr: The 1500−1000 cm^{-1} Frequency Region. If Trp in the triad is the electron donor for the formation of FAD$^{\bullet-}$, the FAD$^{\bullet-}$ minus FAD^{ox} difference FTIR spectrum at 200 K (Figure 5a) also contains the vibrations of Trp$^{\bullet+}$ on the positive side and Trp on the negative side. Previous theoretical calculations of the indolyl radical cation suggested the presence of the normal modes at 1459, 1074, and 1040 cm^{-1}.[37] Thus, the positive peaks at 1489, 1060, and 1046 cm^{-1} in Figure 5a are good candidates for Trp$^{\bullet+}$ vibrations that can be tested by isotopic labeling in the future.

A common peak pair in Figure 5 is observed at 1227 (−)/1215 (+) cm^{-1}, which is upshifted by 3−5 cm^{-1}, not downshifted, in D_2O. When Tyr functions as both a hydrogen bond donor and acceptor, the Tyr vibration exhibits such a characteristic feature for H/D exchange.[38] The frequency change at 200 K for the FAD$^{\bullet-}$ minus FAD^{ox} difference FTIR spectrum (Figure 5a) indicates that this change accompanies the primary electron transfer. The peak pair at 1227 (−)/1215 (+) cm^{-1} is similarly observed in the FADH$^{\bullet}$ minus FAD^{ox} difference FTIR spectrum (Figure 5b), but the amplitude is smaller (46% of Figure 5a). This suggests that the structural change, possibly because of Tyr, is partially relaxed by the subsequent proton transfer. The peak pair is also observed in the FADH^{-} minus FADH$^{\bullet}$ difference FTIR spectrum in Figure 5c, whose amplitude is even smaller (39% of Figure 5a). As a consequence, the amplitude of the peak pair in the FADH^{-} minus FAD^{ox} difference FTIR spectrum (Figure 5d) is 85% of Figure 5a. From these results, two Tyr residues may be involved in the photoactivation reaction, where both change their hydrogen bonding structures from FAD^{ox} to FAD$^{\bullet-}$ but neither is an electron donor. Upon formation of FADH$^{\bullet}$, the structure of one Tyr is preserved, while the other is restored. Then, FADH^{-} formation changes the structures of two Tyr residues again. If instead a Tyr radical were formed, its signal would appear at ∼1500 cm^{-1}.[39,40] Because this signature band of the Tyr radical is not present in these spectra (Figure 5a−d), the data instead provide support for our alternative interpretation.

Secondary Structure Perturbations at 1700−1600 cm^{-1}. Amide I, the C═O stretching vibration of the peptide backbone, appears in this frequency region.[41] The unique spectral features are obtained for each difference FTIR spectrum, and the enlarged spectra are shown in Figure S3 of the Supporting Information. It should be noted that this region contains other vibrations such as those of flavin and/or side chains of proteins. In general, amide I is little influenced by H−D exchange, and the spectral downshift by >3 cm^{-1} in D_2O does not originate from amide I. For instance, the bands at 1688 (−), 1672 (+), and 1666 (+) cm^{-1} in the FAD$^{\bullet-}$ minus FAD^{ox} difference FTIR spectrum (Figure 5a) do not originate from amide I, but those at 1633 (−) and 1625 (+) cm^{-1} may contain amide I vibrations. A previous study showed that the bands at 1688 (−) and 1625 (+) cm^{-1} originate from the C_2═O stretching vibrations of FAD^{ox} and FAD$^{\bullet-}$, respectively.[32] Therefore, the positive band at 1625 cm^{-1} mainly originates from the C_2═O stretching vibration of flavin. However, from the presence of the peak pair at 1633 (−) and 1625 (+) cm^{-1}, and the weak H−D effect for the negative band at 1633 cm^{-1}, it is possible that the FAD$^{\bullet-}$ minus FAD^{ox} difference FTIR spectrum contains the amide I vibration at these frequencies. The peak pair at 1633 (−)/1625 (+) cm^{-1} is characteristic of the amide I vibration of the β-sheet conformation.

The FADH$^{\bullet}$ minus FAD^{ox} difference FTIR spectrum (Figure 5b) shows the negative band at 1690 cm^{-1}, which is most likely to be the C_2═O stretch of FAD.[13,26] Also, a previous study showed that the twin positive peaks at 1663 and 1654 cm^{-1} should comprise the C_2═O stretching vibration for FADH$^{\bullet}$.[32] On the other hand, twin positive peaks at 1663 and 1654 cm^{-1} are insensitive to H/D exchange, though their amplitudes were considerably decreased. Therefore, the bands probably originate from amide I vibrations, with a frequency characteristic of α-helical conformation.[38] Thus, the primary electron transfer (FAD$^{\bullet-}$ formation) is accompanied by structural perturbation of the β-sheet, and the subsequent proton transfer (FADH$^{\bullet}$ formation) increases the level of α-helical conformation.

Figure 5c apparently shows that the FADH^{-} minus FADH$^{\bullet}$ difference FTIR spectrum is highly sensitive to H/D exchange. Nevertheless, it should be noted that the spectral features are similar between H_2O and D_2O. The negative peak at 1661 cm^{-1} is largely reduced in D_2O, but the amplitudes of the peak pairs at 1661 (−)/1645 (+) cm^{-1} in H_2O and 1661 (−)/1643 (+) cm^{-1} in D_2O are similar. This suggests the amide I origin, and the apparent decrease in the magnitude of the negative 1661 cm^{-1} band in D_2O may be due to the baseline drift. The positive peak at 1625 cm^{-1} looks H/D unexchangeable, though the amplitude is decreased. Amide I changes can be more clearly observed in D_2O. Because amide I vibrations at 1660−1650 and 1640−1620 cm^{-1} are characteristic of α-helix and β-sheet, respectively, the secondary electron transfer (FADH^{-} formation) accompanies structural changes that decrease the level of α-helical conformation and increase the level of β-strand conformation in (6−4) PHR. These secondary structural changes of the protein backbone need not be in the same region.

In summary, the primary electron transfer (FAD$^{\bullet-}$ formation) is accompanied by structural perturbation of the β-sheet, but no significant changes in α-helicity. The subsequent proton transfer (FADH$^{\bullet}$ formation) causes a transient increase in α-helicity. Secondary structural rearrangement of an α-helix or α-helices may be needed for the proton to be taken up by FAD. Subsequently, the final electron transfer (FADH^{-} formation) is accompanied by a decreased α-helicity and an increased level of β-strand conformation. As a consequence, when we compare the fully oxidized (FAD^{ox}) and reduced (FADH^{-}) states, there are no changes in α-helicity but significant perturbations in β-sheet conformation.

Structural Similarity of FAD$^{\bullet-}$ and FADH^{-}. Figure 6 compares the FAD$^{\bullet-}$ minus FAD^{ox} (red line) and the FADH^{-} minus FAD^{ox} (black line) spectra, which are reproduced from Figure 5. As one can clearly see, the two spectra are similar, including the amide I vibration. This implies structural similarity between FAD$^{\bullet-}$ and FADH^{-}; these chemical structures of FAD are different but carry negative charge. The FAD$^{\bullet-}$ specific band at 1489 cm^{-1} and the FADH^{-} specific band at 1397 cm^{-1} presumably originate from FAD. A previous study suggested that the bands at 1489 (+) and 1397 (+) cm^{-1} originate from the C═N stretching vibration and the in-plane rocking mode for N_5-H, respectively.[32,42]

In the amide I region, there are common positive peaks at 1674, 1665, 1652, and 1625 cm^{-1} for both FAD$^{\bullet-}$ and FADH^{-}. This observation together with different amide I signals for FADH$^{\bullet}$ and FAD^{ox} (Figure 5b) strongly suggests that the negative charge at the chromophore is important for the structure of (6−4) PHR. In other words, the protein structures of four redox states in (6−4) PHR can be classified into three confomations: FAD^{ox}, FADH$^{\bullet}$, and FAD$^{\bullet-}$/FADH^{-}.

dx.doi.org/10.1021/bi300530x | Biochemistry 2012, 51, 5774−5783

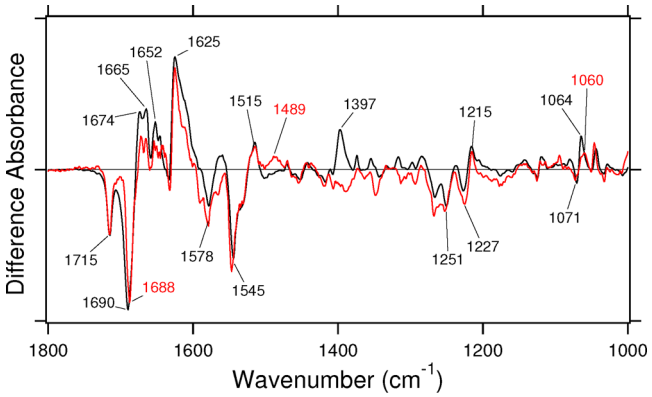

Figure 6. Comparison of the FAD$^{\bullet-}$ minus FAD^{ox} (red) and FADH$^-$ minus FAD^{ox} (black) difference FTIR spectra of *Xenopus* (6–4) PHR, which were reproduced from the black lines in panels a and d of Figure 5, respectively.

Spectral Comparison between (6–4) PHR and CRY-DASH. Despite striking similarities among homologous members of the CRY/PHR family, their functional diversity remains puzzling. We previously reported the FAD$^{\bullet-}$ minus FAD^{ox} and FADH$^-$ minus FAD^{ox} spectra of the DASH-type cryptochrome from *Synechocystis* (CRY-DASH).[18] Because we now have the difference FTIR spectra of the four redox states of *Xenopus* (6–4) PHR, it is intriguing to compare these spectra with those of CRY-DASH. Figure 7 shows overlaid FAD$^{\bullet-}$ minus FAD^{ox} (a) and FADH$^-$ minus FAD^{ox} (b) FTIR spectra for (6–4) PHR (black line) and CRY-DASH (green line).

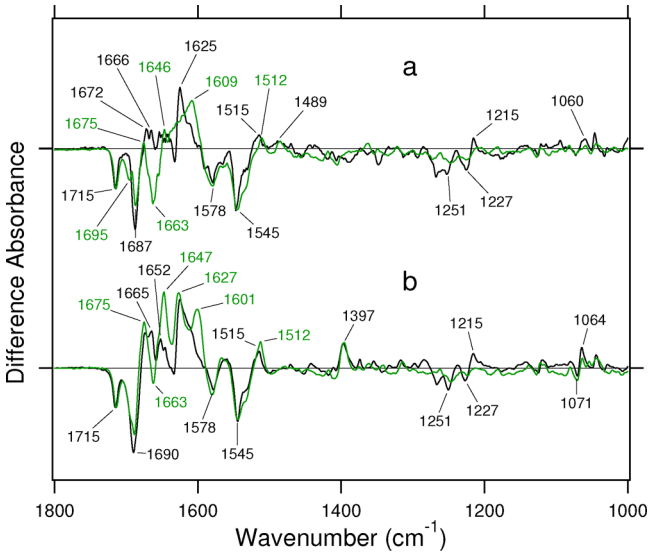

Figure 7. Comparison of light-induced difference FTIR spectra of *Xenopus* (6–4) PHR (black) and SCRY-DASH (green). (a) FAD$^{\bullet-}$ minus FAD^{ox} difference FTIR spectra. (b) FADH$^-$ minus FAD^{ox} difference FTIR spectra.

Negative FAD^{ox} specific peaks at 1715, 1690, 1578, and 1545 cm^{-1} are common between *Xenopus* (6–4) PHR and SCRY-DASH and can be ascribed to the C_4=O, C_2=O, C_{4a}=N_5, and C_{10a}=N_1 stretching vibrations of FAD, respectively.[26−31] Similarly, the FAD$^{\bullet-}$ specific peak at 1489 cm^{-1} for (6–4) PHR is commonly observed for SCRY-DASH (Figure 7a), while the FADH$^-$ specific peak at 1396 cm^{-1} is commonly observed for both (Figure 7b). These bands probably originate from the flavin chromophore, and common peaks for each redox state are reasonable.[18]

In contrast to the conservation of chromophore bands between CRY-DASH and (6–4) PHR, the protein bands are different. The peak pair at 1227 (−)/1215 (+) cm^{-1} for (6–4) PHR, possibly because of Tyr, was not clearly observable for SCRY-DASH. In Raman data of *Vibrio* cryptochrome 1, another type of CRY-DASH, however, the 1227 cm^{-1} band characteristic of FADH$^{\bullet}$ was observed.[43] This suggests that SCRY-DASH does not contain the corresponding Tyr residue. On the basis of sequence and three-dimensional analysis, the possible candidates for the Tyr residues in (6–4) PHR are Y254, Y295, Y296, and Y412.[4,5] To identify the signal, further experiments, such as mutation analysis, are required; however, these tyrosines are 4–8 Å from FAD and are not present in the SCRY-DASH sequence.

A prominent spectral difference can be seen in the amide I region between (6–4) PHR and CRY-DASH. In the case of CRY-DASH, a negative peak at 1663 cm^{-1}, observed for the FAD$^{\bullet-}$ minus FAD^{ox} and FADH$^-$ minus FAD^{ox} spectra (green curve in Figure 7), is unexchangeable for D_2O.[18] This strongly suggests structural perturbation of α-helicity upon formation of FAD$^{\bullet-}$ and FADH$^-$ from FAD^{ox} in CRY-DASH, but not in (6–4) PHR. For the FAD$^{\bullet-}$ state, the 1609 cm^{-1} band for CRY-DASH is much lower in frequency than for (6–4) PHR (1625 cm^{-1}). For the FADH$^-$ state, the peaks at 1675, 1647, 1627, and 1601 cm^{-1} are all insensitive to H/D exchange[18] and thus can be assigned for the amide I vibration. These results suggest that structural changes of the protein are larger in CRY-DASH than in (6–4) PHR and this might reflect the functional difference between the sensor and enzyme.

DISCUSSION

There are four different redox states for the FAD chromophore of PHR: a fully oxidized form (FAD^{ox}), an anion radical form (FAD$^{\bullet-}$), a neutral radical form (FADH$^{\bullet}$), and a fully reduced form (FADH$^-$). The enzymatically active state of PHR is FADH$^-$, and two photons are needed for the activation: FAD^{ox} is first converted to FADH$^{\bullet}$ by light-induced one-electron and one-proton transfers and then to FADH$^-$ by light-induced one-electron transfer. In this work, we studied the detailed activation process of *Xenopus* (6–4) PHR using UV–visible and FTIR spectroscopy. By lowering the temperature (200 K), we successfully trapped FAD$^{\bullet-}$, where electron transfer occurs but proton transfer does not. We then observed FADH$^{\bullet}$ after the subsequent proton transfer reaction via 450 nm illumination at 277 K, where the FADH$^-$ signal in the difference FTIR spectra could be deconvoluted, by using the results from UV–visible spectroscopy. We finally obtained the FAD$^{\bullet-}$ minus FAD^{ox}, FADH$^{\bullet}$ minus FAD^{ox}, and FADH$^-$ minus FAD^{ox} spectra, from which any difference spectrum among the four redox states can be calculated. Detailed structural analysis requires band assignments using isotope labeling and site-directed mutagenesis, as we performed for bacteriorhodopsin[44,45] and the LOV domain,[46,47] while we discuss the molecular mechanism of the activation of (6–4) PHR based on our FTIR results below.

Environment of the Flavin Chromophore in (6–4) PHR. Light-induced difference FTIR spectra contain signals from both the chromophore and the protein. In general, the former is predominant, as has been shown for retinal proteins[48] and LOV domains,[49,50] which is also the case for (6–4) PHRs and CRYs. Frequencies of FAD^{ox} at 1715, 1690, 1578, and 1545

dx.doi.org/10.1021/bi300530x | *Biochemistry* 2012, 51, 5774–5783

cm^{-1} (negative bands in Figure 5a,b,d) can be assigned to the C_4=O, C_2=O, C_{4a}=N_5, and C_{10a}=N_1 stretching vibrations of flavin, respectively.[26−31] The bands at 1489, 1535, and 1397 cm^{-1}, being specific to $FAD^{\bullet-}$, $FADH^{\bullet}$, and $FADH^{-}$, respectively, can also be ascribed to the vibrations of the flavin chromophore. The 1489 cm^{-1} band of $FAD^{\bullet-}$ possibly originates from the C=N stretching vibrations in the isoalloxazine ring,[32] while the ring vibration of $Trp^{\bullet+}$ may also be involved.[37] A previous theoretical study suggested that the 1625 cm^{-1} band of $FAD^{\bullet-}$ (Figure 5a) originates from the C_2=O stretching vibration of flavin. A recent theoretical calculation of lumiflavin (LF) reported that the ring vibration mainly consisting of C=N stretches in isoalloxazine (1545 cm^{-1}) is slightly downshifted in the neutral radical ($LFH^{\bullet}$) and split into two differently downshifted and much weaker bands in the anion radical ($LF^{\bullet-}$).[32] Therefore, the band at 1535 cm^{-1} can be ascribed to the C=N stretching vibration in $FADH^{\bullet}$. The H/D unexchangeable band at 1397 cm^{-1} of $FADH^{-}$ possibly originates from ring vibrations of the flavin chromophore.[51] In fact, this band is observed for $FADH^{-}$ of CRY-DASH (Figure 7). Thus, in the CRY/PHR family, the strong FTIR peaks can be assigned to flavin vibrations. Similar frequencies for FAD between solution and protein environments suggest that the structural properties of the flavin chromophore are maintained in (6−4) PHR.

Electron and Proton Transfer Reactions in (6−4) PHR. Photoactivation of (6−4) PHR is accompanied by electron and proton transfer processes distinct from the DNA repair reaction. The primary electron transfer converts FAD^{ox} into $FAD^{\bullet-}$, followed by a proton transfer to form $FADH^{\bullet}$, and finally $FADH^{-}$ is formed by the secondary electron transfer. There must be two electron donors and one proton donor for activation from FAD^{ox}, whereas none of them has been identified for (6−4) PHR. With regard to the primary electron transfer, an important role of the tryptophan triad chain has been suggested. In the case of *E. coli* CPD PHR, substitution of the most distant Trp of the triad chain disturbs the electron transfer,[7] and (6−4) PHRs structurally conserve the tryptophan triad chain with some modification. The presence of visible absorption at 500−700 nm (Figure 4) and FTIR bands at 1489, 1060, and 1046 cm^{-1} (Figure 5a) suggests the involvement of radical species, possibly $Trp^{\bullet+}$.

One proton is gained by flavin in the conversion from $FAD^{\bullet-}$ to $FADH^{\bullet}$. Successful isolation of the primary electron transfer and proton transfer at 200 K implies that the proton transfer is accompanied by conformational changes in the protein. Protonated carboxylic acids are good candidates for the donor of the proton to the FAD, and in fact, a negative FTIR band observed at 1735 cm^{-1} suggested that a carboxylic acid is the FAD proton donor for photoreduction of plant CRY.[35] However, Figure 5 shows the absence of such bands for (6−4) PHR, indicating that protonated carboxylic acid is not the proton donor. Consistent with the FTIR results, plant CRY anchors the redox-active FAD N_5 position with a hydrogen bond to the carboxylic acid Asp,[35] whereas PHRs conserve this position as Asn.[5] At present, the proton donor and secondary electron donor to FAD in (6−4) PHR remain to be identified. It should be noted that unlike other CRY/PHR family members, including CRY-DASH, (6−4) PHR can form $FADH^{-}$ stably without a reducing agent such as DTT, implying that light energy is sufficient for overcoming the potential barrier for forming $FADH^{-}$. Although the identification of the proton and secondary electron donors awaits further investigation, our FTIR spectra provide the analytical basis of future study.

Secondary Structural Changes during the Activation of (6−4) PHR. The structure of (6−4) PHR has a typical CRY/PHR fold, consisting of an N-terminal α/β domain and a C-terminal α-helical domain, containing the active site FAD. Our spectral analysis of the amide I vibration reveals that the primary electron transfer ($FAD^{\bullet-}$ formation) in *Xenopus* (6−4) PHR is accompanied by perturbation of the β-sheet conformation, but no significant changes in α-helicity. The subsequent proton transfer ($FADH^{\bullet}$ formation) causes a transient increase in α-helicity that is reversed by the secondary electron transfer ($FADH^{-}$ formation), which also enhances the β-sheet conformation. As a consequence, when we compare fully oxidized (FAD^{ox}) and reduced ($FADH^{-}$) states, there are no significant changes for α-helicity, but more noticeable perturbation for the β-sheet conformation. Small changes in α-helicity in (6−4) PHR may be characteristic of activation of this enzyme.

Relatively small structural changes for (6−4) PHR are supported by the spectral resemblance between the $FAD^{\bullet-}$ minus FAD^{ox} (200 K) and $FADH^{-}$ minus FAD^{ox} (277 K) difference FTIR spectra (Figure 6). At 200 K, protein structural changes are limited compared to those of higher temperatures, whereas similar spectra, particularly on the amide I bands, suggest local structural perturbation around the FAD chromophore. The lack of the signal in the α-helix for (6−4) PHR, unlike CRY-DASH, in Figure 7 may also support this argument. In the previous paper, we compared the $FADH^{-}$ minus FAD^{ox} spectra in the absence and presence of oligonucleotides containing the (6−4) photoproduct.[13] Although the two spectra were very similar, we reported an additional negative peak at 1653 cm^{-1} only in the presence of the damaged DNA. This suggests that structural perturbation takes place only in the DNA-bound form of (6−4) PHR. The spectral analysis for the photoactivation in the presence of the (6−4) photoproduct is thus intriguing. In addition, one might expect the possibility that $FAD^{\bullet-}$ could have DNA repair activity, because of the structural similarity between $FAD^{\bullet-}$ and $FADH^{-}$.

CONCLUSION

We examined different FAD redox states of (6−4) PHR by UV−visible and FTIR spectroscopy and successfully obtained difference FTIR spectra among four redox states of FAD. Spectral analysis of the C=O stretching vibration of protonated carboxylic acids shows the lack of the signal upon the proton transfer reaction, implying that carboxylic acids are not proton donors. The involvement of structural changes in Trp and Tyr is suggested by the UV−visible and FTIR analysis of $FAD^{\bullet-}$. The spectral analysis of the amide I vibration reveals that the primary electron transfer ($FAD^{\bullet-}$ formation) is accompanied by perturbation of the β-sheet conformation, but not α-helicity. The subsequent proton transfer ($FADH^{\bullet}$ formation) causes a transient increase in α-helicity that is reversed by the secondary electron transfer ($FADH^{-}$ formation), which also perturbs the β-sheet conformation. On the basis of the obtained difference FTIR spectra, isotope labeling and various mutants of (6−4) PHR will provide a detailed molecular mechanism for the photoactivation of this enzyme.

dx.doi.org/10.1021/bi300530x | *Biochemistry* 2012, 51, 5774−5783

■ ASSOCIATED CONTENT

Supporting Information

FTIR spectral comparison of the present His-tagged sample in this study and the previous sample preparation using the GST tag[13] for the photoactivation and photorepair process (Figure S1), an estimate of the possible involvement of $FADH^{\bullet}$ as the product upon formation of $FAD^{\bullet-}$ at 200 K in Figure 4 (Figure S2), and an expanded view of Figure 5 at 1800−1350 cm^{-1} (Figure S3). This material is available free of charge via the Internet at http://pubs.acs.org.

■ AUTHOR INFORMATION

Corresponding Author

*Department of Frontier Materials, Nagoya Institute of Technology, Showa-ku, Nagoya 466-8555, Japan. Phone and fax: 81-52-735-5207. E-mail: kandori@nitech.ac.jp.

Funding

This work was supported by grants from the Japanese Ministry of Education, Culture, Sports, Science, and Technology to H.K. (20050015 and 20108014) and National Institutes of Health Grant GM37684 to E.D.G. K.H. was supported by the Skaggs Institute for Chemical Biology.

Notes

The authors declare no competing financial interest.

■ ABBREVIATIONS

PHR, photolyase; CPD, cyclobutane pyrimidine dimer; (6−4) PP, (6−4) photoproduct; FAD, flavin adenine dinucleotide; FTIR, Fourier-transform infrared; FAD^{ox}, fully oxidized form of FAD; $FADH^{-}$, fully reduced form of FAD; $FADH^{\bullet}$, neutral semiquinoid form of FAD; $FAD^{\bullet-}$, anion radical form of FAD; CRY, cryptochrome; UV−visible, ultraviolet−visible; DTT, dithiothreitol.

■ REFERENCES

(1) Sancar, A. (2003) Structure and function of DNA photolyase and cryptochrome blue-light photoreceptors. *Chem. Rev. 103*, 2203−2237.

(2) Weber, S. (2005) Light-driven enzymatic catalysis of DNA repair: A review of recent biophysical studies on photolyase. *Biochim. Biophys. Acta 1707*, 1−23.

(3) Todo, T., Takemori, H., Ryo, H., Ihara, M., Matsunaga, T., Nikaido, O., Sato, K., and Nomura, T. (1993) A new photoreactivating enzyme that specifically repairs ultraviolet light-induced (6−4) photoproducts. *Nature 361*, 371−374.

(4) Maul, M. J., Barends, T. R., Glas, A. F., Cryle, M. J., Domratcheva, T., Schneider, S., Schlichting, I., and Carell, T. (2008) Crystal structure and mechanism of a DNA (6−4) photolyase. *Angew. Chem., Int. Ed. 47*, 10076−10080.

(5) Hitomi, K., DiTacchio, L., Arvai, A. S., Yamamoto, J., Kim, S. T., Todo, T., Tainer, J. A., Iwai, S., Panda, S., and Getzoff, E. D. (2009) Functional motifs in the (6−4) photolyase crystal structure make a comparative framework for DNA repair photolyases and clock cryptochromes. *Proc. Natl. Acad. Sci. U.S.A. 106*, 6962−6967.

(6) Hitomi, K., Kim, S. T., Iwai, S., Harima, N., Otoshi, E., Ikenaga, M., and Todo, T. (1997) Binding and catalytic properties of *Xenopus* (6−4) photolyase. *J. Biol. Chem. 272*, 32591−32598.

(7) Aubert, C., Vos, M. H., Mathis, P., Eker, A. P., and Brettel, K. (2000) Intraprotein radical transfer during photoactivation of DNA photolyase. *Nature 405*, 586−590.

(8) Kim, S. T., Li, Y. F., and Sancar, A. (1992) The third chromophore of DNA photolyase: Trp-277 of *Escherichia coli* DNA photolyase repairs thymine dimers by direct electron transfer. *Proc. Natl. Acad. Sci. U.S.A. 89*, 900−904.

(9) Todo, T., Kim, S. T., Hitomi, K., Otoshi, E., Inui, T., Morioka, H., Kobayashi, H., Ohtsuka, E., Toh, H., and Ikenaga, M. (1997) Flavin adenine dinucleotide as a chromophore of the *Xenopus* (6−4) photolyase. *Nucleic Acids Res. 25*, 764−768.

(10) Kandori, H. (2000) Role of internal water molecules in bacteriorhodopsin. *Biochim. Biophys. Acta 1460*, 177−191.

(11) Kötting, C., and Gerwert, K. (2005) Proteins in action monitored by time-resolved FTIR spectroscopy. *ChemPhysChem 6*, 881−888.

(12) Noguchi, T. (2007) Light-induced FTIR difference spectroscopy as a powerful tool toward understanding the molecular mechanism of photosynthetic oxygen evolution. *Photosynth. Res. 91*, 59−69.

(13) Zhang, Y., Iwata, T., Yamamoto, J., Hitomi, K., Iwai, S., Todo, T., Getzoff, E. D., and Kandori, H. (2011) FTIR study of light-dependent activation and DNA repair processes of (6−4) photolyase. *Biochemistry 50*, 3591−3598.

(14) Berndt, A., Kottke, T., Breitkreuz, H., Dvorsky, R., Hennig, S., Alexander, M., and Wolf, E. (2007) A novel photoreaction mechanism for the circadian blue light photoreceptor *Drosophila* cryptochrome. *J. Biol. Chem. 282*, 13011−13021.

(15) Kao, Y.-T., Tan, C., Song, S.-H., Öztürk, N., Li, J., Wang, L., Sancar, A., and Zhong, D. (2008) Ultrafast dynamics and anionic active states of the flavin cofactor in cryptochrome and photolyase. *J. Am. Chem. Soc. 130*, 7695−7701.

(16) Öztürk, N., Song, S.-H., Selby, C. P., and Sancer, A. (2008) Animal type 1 cryptochromes. *J. Biol. Chem. 283*, 3256−3263.

(17) Hitomi, K., Okamoto, K., Daiyasu, H., Miyashita, H., Iwai, S., Toh, H., Ishiura, M., and Todo, T. (2000) Bacterial cryptochrome and photolyase: Characterization of two photolyase-like genes of *Synechocystis* sp. PCC6803. *Nucleic Acids Res. 28*, 2353−2362.

(18) Iwata, T., Zhang, Y., Hitomi, K., Getzoff, E. D., and Kandori, H. (2010) Key dynamics of conserved asparagine in a cryptochrome/photolyase family protein by Fourier transform infrared spectroscopy. *Biochemistry 49*, 8882−8891.

(19) Zhang, Y., Yamamoto, J., Yamada, D., Iwata, T., Hitomi, K., Todo, T., Getzoff, E. D., Iwai, S., and Kandori, H. (2011) Substrate assignment of the (6−4) photolyase reaction by FTIR spectroscopy. *J. Phys. Chem. Lett. 2*, 2774−2777.

(20) Iwata, T., Yamamoto, A., Tokutomi, S., and Kandori, H. (2007) Hydration and temperature similarly affects light-induced protein structural changes in the chromophore domain of phototropin. *Biochemistry 46*, 7016−7021.

(21) Yamamoto, A., Iwata, T., Tokutomi, S., and Kandori, H. (2008) Role of Phe1010 in light-induced structural changes of the neo1-LOV2 domain of *Adiantum*. *Biochemistry 47*, 922−928.

(22) Schleicher, E., Hitomi, K., Kay, C. W. M., Getzoff, E. D., Todo, T., and Weber, S. (2007) Electron nuclear double resonance differentiates complementary roles for active site histidines in (6−4) photolyase. *J. Biol. Chem. 282*, 4738−4747.

(23) Langenbacher, T., Immeln, D., Dick, B., and Kottke, T. (2009) Microsecond light-induced proton transfer to flavin in the blue light sensor plant cryptochrome. *J. Am. Chem. Soc. 131*, 14274−14280.

(24) Offenbacher, A. R., Vassiliev, I. R., Seyedsayamdost, M. R., Stubbe, J., and Barry, B. A. (2009) Redox-linked structural changes in ribonucleotide reductase. *J. Am. Chem. Soc. 131*, 7496−7497.

(25) Solar, S., Surdhar, N. G. P. S., Armstrong, D. A., and Singh, A. (1991) Oxldatlon of tryptophan and N-methylindole by $N_3^{\bullet}$, Br_2^{-}, and $(SCN)_2^{-}$ radlcals in light- and heavy-water solutions: A pulse radiolysis study. *J. Phys. Chem. 95*, 3639−3643.

(26) Wille, G., Ritter, M., Friedemann, R., Möntele, W., and Hübner, G. (2003) Redox-triggered FTIR difference spectra of FAD in aqueous solution and bound to flavoproteins. *Biochemistry 42*, 14814−14821.

(27) Bowman, W. D., and Spiro, T. G. (1981) Normal mode analysis of lumiflavin and interpretation of resonance Raman spectra of flavoproteins. *Biochemistry 20*, 3313−3318.

(28) Schmidt, J., Coudron, P., Thompson, A. W., Watters, K. L., and McFarland, J. T. (1983) Assignment and the effect of hydrogen bonding on the vibrational normal modes of flavins and flavoproteins. *Biochemistry 22*, 76−84.

(29) Abe, M., and Kyogoku, Y. (1987) Vibrational analysis of flavin derivatives: Normal coordinate treatments of lumiflavin. *Spectrochim. Acta 43A*, 1027−1038.
(30) Livery, C. R., and McFarland, J. T. (1990) Assignment and the effect of hydrogen bonding on the vibrational normal modes of flavins and flavoproteins. *J. Phys. Chem. 94*, 3980−3994.
(31) Zhang, W., Vivoni, A., Lombard, J. R., and Birke, R. L. (1995) Time-resolved SERS study of direct photochemical charge transfer between FMN and a Ag electrode. *J. Phys. Chem. 99*, 12846−12857.
(32) Rieff, B., Bauer, S., Mathias, G., and Tavan, P. (2011) IR spectra of flavins in solution: DFT/MM description of redox effects. *J. Phys. Chem. B 115*, 2117−2123.
(33) Li, J., Uchida, T., Ohta, T., Todo, T., and Kitagawa, T. (2006) Characteristic structure and environment in FAD cofactor of (6−4) photolyase along function revealed by resonance Raman spectroscopy. *J. Phys. Chem. B 110*, 16724−16732.
(34) Barth, A. (2000) The infrared absorption of amino acid side chains. *Prog. Biophys. Mol. Biol. 74*, 141−173.
(35) Kottke, T., Batschauer, A., Ahmad, M., and Heberle, J. (2006) Blue-light-induced changes in *Arabidopsis* cryptochrome 1 probed by FTIR difference spectroscopy. *Biochemistry 45*, 2472−2479.
(36) Brautigam, C. A., Smith, B. S., Ma, Z., Palnitkar, M., Tomchick, D. R., Machius, M., and Deisenhofer, J. (2004) Structure of the photolyase-like domain of cryptochrome 1 from *Arabidopsis thaliana*. *Proc. Natl. Acad. Sci. U.S.A. 101*, 12142−12147.
(37) Walden, S. E., and Wheeler, R. A. (1996) Structural and vibrational analysis of indolyl radical and indolyl radical cation from density functional methods. *J. Chem. Soc., Perkin Trans. 2,*, 2663−2672.
(38) Takahashi, R., Okajima, K., Suzuki, H., Nakamura, H., Ikeuchi, M., and Noguchi, T. (2007) FTIR study on the hydrogen bond structure of a key tyrosine residue in the flavin-binding blue light sensor TePixD from Thermosynechococcus elongates. *Biochemistry 46*, 6459−6467.
(39) Berthomieu, C., and Boussac, A. (1995) FTIR and EPR study of radical of aromatic amino acids 4-methylimidazole and phenol generated by UV irradiation. *Biospectroscopy 1*, 187−206.
(40) Noguchi, T., Inoue, Y., and Tang, X. S. (1997) Structural coupling between the oxygen-evolving Mn cluster and a tyrosine residue in photosystem II as revealed by fourier transform infrared spectroscopy. *Biochemistry 36*, 14705−14711.
(41) Krimm, S., and Bandekar, J. (1986) Vibrational spectroscopy and conformation of peptides, polypeptides, and proteins. *Adv. Protein Chem. 38*, 181−364.
(42) Schleicher, E., Hessling, B., Illarionova, V., Bacher, A., Weber, S., Richter, G., and Gerwert, K. (2005) Light-induced reactions of *Escherichia coli* DNA photolyase monitored by Fourier transform infrared spectroscopy. *FEBS J. 272*, 1855−1866.
(43) Sokolowsky, K., Newton, M., Lucero, C., Wertheim, B., Freedman, J., Cortazar, F., Czochor, J., Schelvis, J. P. M., and Gindt, Y. M. (2010) Spectroscopic and Thermodynamic Comparisons of *Escherichia coli* DNA Photolyase and *Vibrio cholerae* Cryptochrome 1. *J. Phys. Chem. B 114*, 7121−7130.
(44) Kandori, H., Kinoshita, N., Yamazaki, Y., Maeda, A., Shichida, Y., Needleman, R., Lanyi, J. K., Bizounok, M., Herzfeld, J., Raap, J., and Lugtenburg, J. (2000) Local and distant protein structural changes on photoisomerization of the retinal in bacteriorhodopsin. *Proc. Natl. Acad. Sci. U.S.A. 97*, 4643−4648.
(45) Tanimoto, T., Shibata, M., Belenky, M., Herzfeld, J., and Kandori, H. (2004) Altered hydrogen bonding of Arg82 during the proton pump cycle of bacteriorhodopsin: A low-temperature polarized FTIR spectroscopic study. *Biochemistry 43*, 9439−9447.
(46) Iwata, T., Nozaki, D., Sato, Y., Sato, K., Nishina, Y., Shiga, K., Tokutomi, S., and Kandori, H. (2006) Identification of the C═O stretching vibrations of FMN and peptide backbone by ^{13}C-labeling of the LOV2 domain of *Adiantum* phytochrome3. *Biochemistry 45*, 15384−15391.
(47) Koyama, T., Iwata, T., Yamamoto, A., Sato, Y., Matsuoka, D., Tokutomi, S., and Kandori, H. (2009) Different role of the Jα helix in the light-induced activation of the LOV2 domains in various phototropins. *Biochemistry 48*, 7621−7628.
(48) Siebert, F. (1995) Infrared spectroscopy applied to biochemical and biological problems. *Methods Enzymol. 246*, 501−526.
(49) Kottke, T., Hegemann, P., Dick, B., and Heberle, J. (2006) The photochemistry of the light-, oxygen-, and voltage-sensitive domains in the algal blue light receptor phot. *Biopolymers 82*, 373−378.
(50) Iwata, T., Tokutomi, S., and Kandori, H. (2011) Light-induced structural changes of the LOV2 domains in various phototropins revealed by FTIR spectroscopy. *Biophysics 7*, 89−98.
(51) Zheng, Y., Carey, P. R., and Palfey, B. A. (2004) Raman spectrum of fully reduced flavin. *J. Raman Spectrosc. 35*, 521−524.